Reservoir Monitoring Using Multi-Geophysical Survey Techniques

T. Ishido[1], K. Goko[2], T. Tosha[1], M. Adachi[3], J. Ishizaki[4], and Y. Nishi[1]

[1]Reservoir Dynamics RG, Geological Survey of Japan / AIST
Central 7, 1-1-1 Higashi, Tsukuba 305-8567, Japan
[2]Nittetsu Kagoshima Geothermal Co.
[3]Okuaizu Geothermal Co.
[4]Tohoku Electric Power Co., Inc.

Keywords

Reservoir management, microgravity, self-potential, history-matching

ABSTRACT

During 2002, we undertook a new cooperative research program entitled *"System Integration of Various Geophysical Measurements for Reservoir Monitoring"* involving both the Okuaizu and Ogiri geothermal fields in Japan. This continuing work carries forward a completed 1997–2002 NEDO/GSJ project. To appraise the utility of reservoir monitoring by simultaneous continuous/repeat measurements of gravity and SP for history-matching of reservoir models, we performed numerical simulations based upon a hypothetical 3D reservoir model and calculated changes in microgravity and self-potential on the ground surface caused by changing reservoir conditions. The results show that combining long-term repeat microgravity surveys with continuous SP measurements taken when the field is shut-in for maintenance can provide useful additional constraints for history-matching studies.

Introduction

Numerical models of geothermal reservoirs are never precise, owing to the problem of non-uniqueness. The difficulty increases as the amount of available relevant field data becomes smaller. If only a few facts are known about the reservoir, a variety of theoretical reservoir models may explain these known facts equally well, but yield very different predictions of future potential. As the amount of field data available increases, of course, these uncertainties diminish. Thus, as time goes on, the understanding of the reservoir improves and forecasts become more reliable. Typically, the data base upon which numerical reservoir models are constructed consists of (1) geophysical surveys of various types, usually performed prior to development, (2) geological interpretations of underground structure, (3) downhole pressure and temperature surveys in shut-in wells, (4) flowing downhole surveys in wells, and (5) pressure-transient test results. Once exploitation begins in earnest, additional data become available, such as temporal trends in downhole flowing pressures and wellhead enthalpies. These latter data may be used in "history-matching" studies. Since the uncertainty in the predictions of numerical reservoir models is directly related to the amount of field data available against which the models can be tested, the addition of repeat geophysical survey data to the above list of pertinent field measurements is likely to improve the reliability of the forecasts. It is well known in this connection that repeat precision gravity surveying has considerable promise for appraising the volumetric properties of any proposed mathematical reservoir model (Ishido et al., 1995).

The application of improved geophysical and geochemical techniques to reservoir management was among the objectives of a geothermal R&D project (*"Development of Technology for Reservoir Mass and Heat Flow Characterization"*) which was carried out by NEDO (the New Energy and Industrial Technology Development Organization) as a part of METI's New Sunshine Program from 1997 through 2002 (e.g. Horikoshi et al., 2001; Yamasawa et al., 2001). GSJ (the Geological Survey of Japan) carried out supporting basic research in cooperation with NEDO, pursuing the development of improved field survey techniques and associated modeling studies involving geophysical survey techniques and their application to reservoir performance monitoring. In addition to gravity monitoring, these techniques included repeat self-potential, resistivity, and seismic velocity surveys.

In 2002, GSJ started a new cooperative research program, *"System Integration of Various Geophysical Measurements for Reservoir Monitoring"*, focused on the Okuaizu and Ogiri areas in Japan, to make practical applications of the results of the NEDO/GSJ project. As a preliminary feasibility study, we first performed numerical simulations based upon a hypothetical 3D reservoir model to appraise reservoir monitoring by simultaneous continuous/repeat measurements of gravity and SP for history-matching of reservoir models.

Reservoir Description

We consider the 3 km × 1.5 km × 2 km volume shown in Figure 1. The computational grid consists of 360 blocks (12 × 3 × 10). Four rock formations (*A*, *B*, *C* and *D*) are present, which differ in porosity and permeability. Other formation properties are uniform: rock grain density is 2600 kg/m^3, rock heat capacity is 1 kJ/kg-°C, and thermal conductivity is 2 W/m-°C. Relative permeabilities are simple straight-line functions with residual water and steam saturations of 30% and 5% respectively. The high-permeability reservoir (*A* in Figure 1) is sandwiched by wall rocks (*D*) and overlain by the low-permeability altered caprock (*C*). At depth, a source of high-temperature (320°C) *"magmatic water"* (tagged with a dilute tracer) is imposed at the southeastern part of the bottom surface. The hot fluid recharges the reservoir and then flows outward toward the northwest through a less permeable formation (*B*). All vertical boundaries except a part of the northwestern surface are impermeable and insulated. Pressure and temperature are maintained at 30–40 bars and 80°C respectively along the top boundary (which is located at 0.5 km depth). Most of the bottom surface (at 2.5 km depth) is impermeable, but constant temperature (320°C) is imposed over the reservoir bottom surface. Any *"fresh water"* which flows downward into the grid through the top surface contains a dilute tracer to permit its identification. For the "EKP-postprocessor" calculations described in the next section, the *"magmatic"* and *"fresh"* waters are assumed to have NaCl concentrations of 0.3 and 0.017 mol/L respectively.

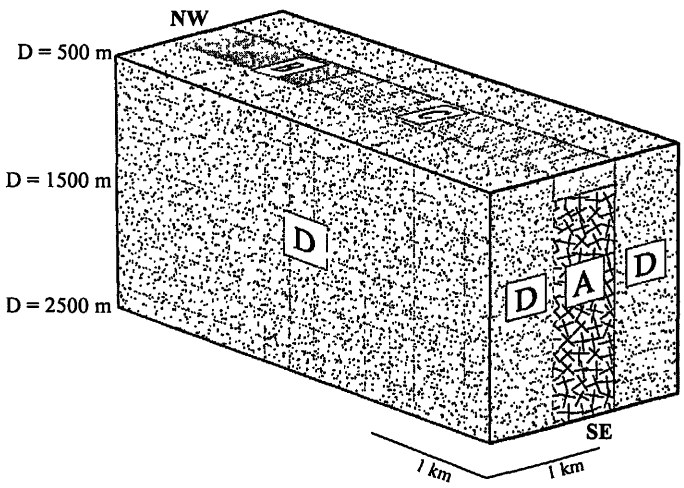

Figure 1. Three-dimensional hypothetical reservoir model. A high permeability reservoir (A) is sandwiched by wall rocks (D) and overlain by a cap rock (C). Deep natural hot water recharge is assumed at the southeastern ("SE") base of the reservoir. The hot fluid rises and leaves the reservoir to the northwest ("NW") through a less permeable formation (B).

We consider four variations of the above model: *"H-P"* (high *k*, porous), *"H-F"* (high *k*, fractured), *"L-P"* (low *k*, porous) and *"L-F"* (low *k*, fractured). Although all of these models have the same common features described above, the permeabilities of formations *A*, *B*, *C* and *D* and the rate of deep hot-fluid recharge for the *"L"* models are only one-tenth of those for the *"H"* models (for which the permeabilities are listed in Table 1 and the recharge rate is 40 kg/sec). Formation *A*, representing the reservoir, is assumed to be a "MINC" double-porosity medium (with fracture zone volume fraction $\psi = 0.05$, fracture zone porosity $\phi_f = 0.1$, matrix region porosity $\phi_m = 0.1$, matrix region permeability $k_m = 10^{-18}$ m^2, and fracture spacing $\lambda = 30$ m) for the *"F"* models, and is treated as equivalent porous medium for the *"P"* models.

Table 1. Rock porosities and permeabilities (*"H"* models).

Formation	Porosity	Permeability (md)		
	ϕ	k_x	k_y	k_z
A (reservoir)	0.10	100.0	10.0	10.0
B	0.05	30.0	10.0	10.0
C (caprock)	0.05	0.1	0.1	0.1
D	0.05	3.0	3.0	3.0

The development of the hydrothermal convection system was computed for the *"H-P"* and *"L-P"* models using the STAR geothermal reservoir simulator (Pritchett, 1995). The system reached quasi-steady state after around 10,000 years of evolution (Figure 2). In the *"H-P"* model, a two-phase steam/water zone develops at shallow levels of the reservoir below the caprock.

The STAR simulator was next used to perform a 4-year forecast of the consequences of production, starting from the natural-states for the *"P"* models described above as the initial conditions. All boundary conditions and rock properties are the same as those used to calculate the natural-states. Fluid is withdrawn from six production wells at a fixed rate of ~100 tons/hour each (total rate of ~600 tons/hour). No re-injection of waste fluid takes place in these calculations. Temperature, pressure, mass flux and the two-phase steam/water zone after ~4 years of field operation are shown in Figure 2 for the *"P"* models.

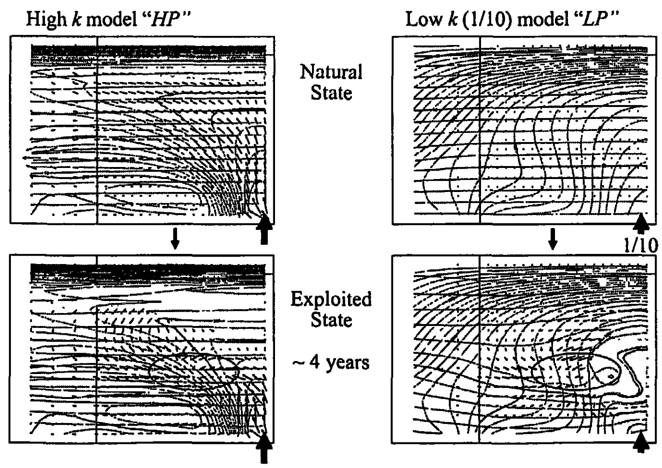

Figure 2. Distributions of temperature (contour interval 10°C), pressure (contour interval 10 bars), mass flux and the two-phase region (shaded area) under natural-state (upper) and exploited (lower) conditions for the "H-P" (left) and "L-P" (right) models. Feedpoints for six production wells are located within the ellipse.

The temporal variations of reservoir pressure caused by field operation are shown in Figure 3. In the calculations, the field is shut in for three months after ~1 and ~3 years of operation. As pressure decreases, the total volume occupied by steam in the reservoir increases from 0.6 × 10^7 m^3 under natural-state conditions to 2.2 × 10^7 and 1.3 × 10^7 m^3 after four years for the *"H-P"*

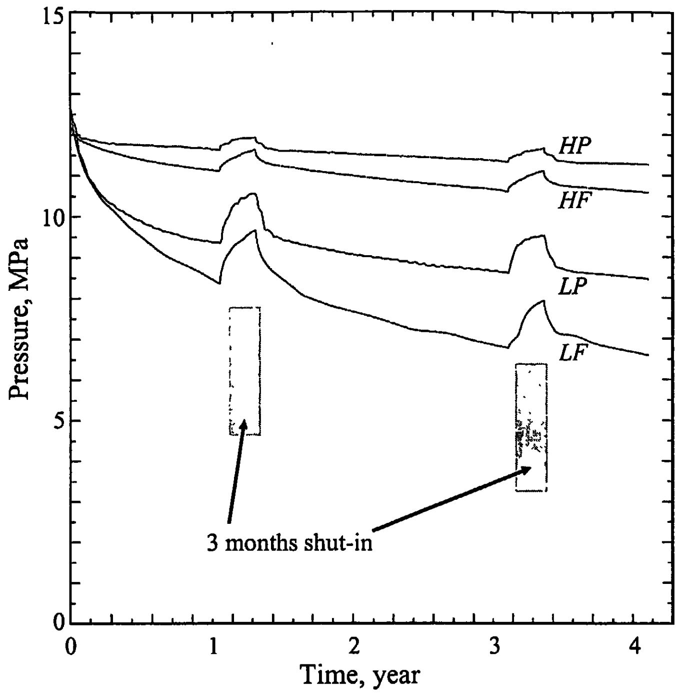

Figure 3. Pressure histories in an observation well located near the boundary between the "A" and "B" formations for the "H-P", "H-F", "L-P" and "L-F" models.

and *"H-F"* models respectively, and from zero to 2.1×10^7 and 1.8×10^7 m^3 for the *"L-P"* and *"L-F"* models respectively. The produced fluid enthalpy is almost constant during the whole 4-year period except for the *"L-F"* model, which exhibits "excess enthalpy" after ~2 years of field operation.

Changes in Microgravity and Self-Potential

Next, STAR's "gravity" and "EKP" postprocessors (see, e.g. Pritchett, 1995; Ishido and Pritchett, 1999; Ishido and Pritchett, 2003) were used to calculate the gravity and self-potential changes at the earth surface which are caused by changes in underground conditions that result from production. Figure 4 shows temporal changes in gravity and self-potential at a station located in the central production area.

The magnitude of gravity decrease is larger for the *"H-P"* model than that for the *"H-F"* model. This is because the total volume of steam created due to production-induced pressure decrease is larger for *"H-P"* than that for *"H-F"* as mentioned above. For the latter model, although the two-phase zone extends deeper and the vapor saturation (S_V) becomes very high in the fracture zone, S_V in the matrix region remains near zero for four years. The total volume of induced steam is similar for the *"L-P"* and *"L-F"* models and larger than for the *"H-P"* model (since the recharge from reservoir boundaries is negligible in the low permeability models). The intermediate magnitude of gravity decrease for the *"L"* models is due to the relatively deep location of the induced two-phase zone, as shown in Figure 2. For all four models, the rate of gravity decrease is reduced during the periods of field wide shut-in, but unlike pressure (Figure 3) no actual recovery is seen.

Self-potential (SP) in the production area is positive under natural-state conditions and decreases rapidly after production begins for all models (Figure 4). Figure 5 shows a vertical section of the electrical potential distribution under natural-state conditions for the *"H"* models (the distribution for the *"L"* models is quite similar). Positive charge accumulates at shallow levels of the reservoir due to the high temperature upflow, which has less capacity to carry positive charge along the flow direction via electrokinetic coupling as temperature decreases (due to lower magnitude of the zeta potential; e.g. Ishido and Pritchett, 1999).

Exploitation drastically changes the SP distribution, as shown in Figure 6, overleaf. Downward liquid flow in the production-induced boiling zone causes corresponding drag currents, resulting

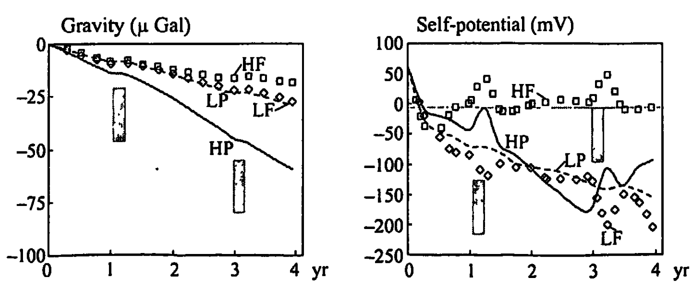

Figure 4. Changes in gravity and SP in the production area, calculated by applying the "mathematical postprocessors" to production-induced changes in reservoir conditions. In principle the "H-P", "H-F", "L-P" and "L-F" models can be distinguished based upon long- and short-term gravity and SP changes.

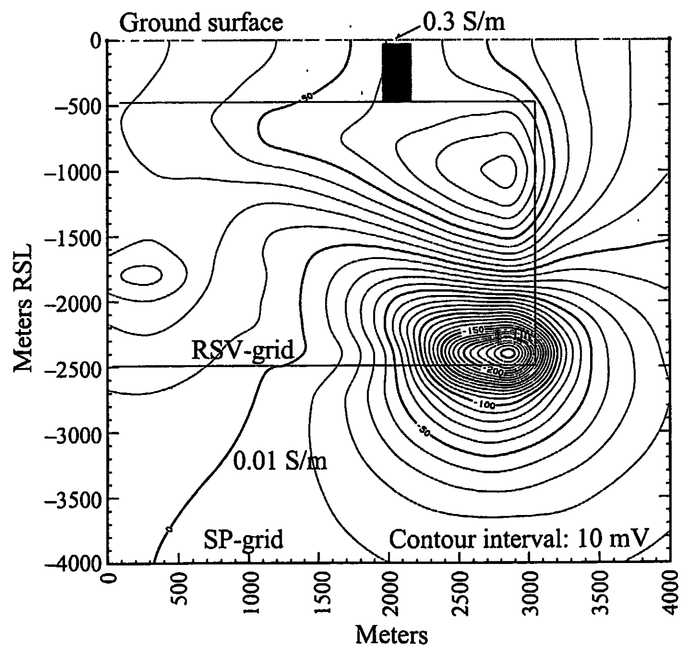

Figure 5. Cross-section of electric potential distribution under natural-state conditions for the "H-P" model. The reservoir simulation grid denoted as "RSV" is embedded in the "SP"-grid, which has a larger spatial extent than the "RSV"-grid. Within the portion of the "SP"-grid overlapped by the "RSV"-grid, the distribution of electrical conductivity is obtained directly from "RSV"-grid values. Elsewhere within the "SP"-grid, the electrical conductivity is assumed to be 0.01 S/m except the shaded zone between the ground surface and the top of "RSV"-grid (0.3 S/m). "EKP-postprocessor" calculation procedure is described by Ishido and Pritchett (1999).

in negative potentials at shallower levels. Although a large subsurface positive potential appears associated with the production zone, it is confined within the region where pressure decreases in the cases of the *"H-P"* and *"H-F"* models. In both cases, the potential anomalies become quite weak by the end of the 3-month shut-in due to changing reservoir conditions (the bottom of two-phase zone moves upward with the shrinkage of the boiling zone, and the production zone pressure nearly recovers to the initial level). Because of the decreasing magnitude of the negative source, surface SP increases significantly during the shut-in as shown in Figure 4 (and actually becomes positive in the *"H-F"* case).

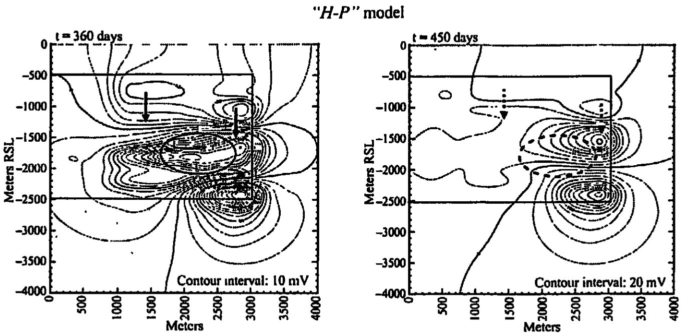

Figure 6. Cross-section of electric potential distribution under exploitation conditions for the "H-P" model. A three-month shut-in takes place from t = 360 to t = 450 days. Ellipse: production zone. Arrows: drag current associated with the liquid-phase downflow in the boiling zone.

In the case of the *"L"* models, the production zone is not overlain by the boiling zone and the influence of the positive potential can be transferred to the ground surface in the presence of a boundary separating regions of smaller (shallower) and larger (deeper) streaming potential coefficient magnitudes, which is associated with the vertical temperature gradient (see e.g. Ishido and Pritchett, 1999). The change in the SP distribution due to fluid production is caused by a combination of this positive source and the downward drag current in the deep boiling zone (Figure 7). In the *"L-F"* model, SP actually decreases during shut-in as shown in Figure 4. This is because of rapid disappearance of the positive source and sustained downward liquid flow through the matrix region.

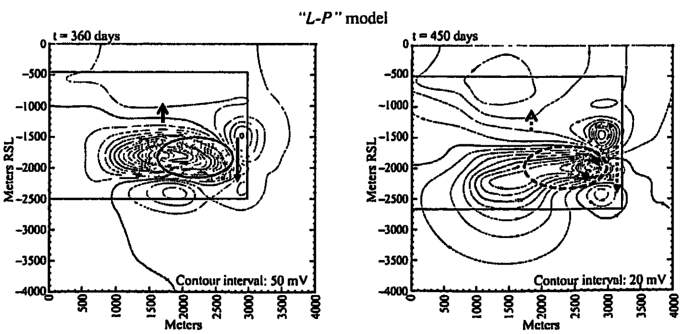

Figure 7. Cross-section of electric potential distribution under exploitation conditions for the "L-P" model. A three-month shut-in takes place from t = 360 to t = 450 days. Ellipse: production zone. Downward arrow: drag current associated with the liquid-phase downflow in the boiling zone. Upward arrow: dipole current source of "total potential" (see, e.g. Ishido and Pritchett, 1999) due to pressure decrease, which appears at a boundary between regions of different streaming potential coefficient.

Reservoir Monitoring Using Gravity And SP Measurements Simultaneously

If the above four models were candidates to represent a real reservoir, what kinds of data would be useful to choose the best model among them? Temperature distribution data under natural-state conditions (from a number of wells) and pressure histories during exploitation conditions (from observation wells) would be helpful to distinguish the *"H"* and *"L"* models. Although production wellhead enthalpy histories are often valuable to distinguish *"P"* and *"F"* models, this is effective only for the *"L"* models in the present case (since only the *"L-F"* model exhibits "excess enthalpy" as mentioned above).

As seen in Figure 4, the histories of gravity and of self-potential at the earth surface are quite different among the four models. *"H-P"* can be distinguished from other three models based on long-term gravity changes. If long-term SP change data are available in addition to gravity changes, *"H-F"* can be distinguished from the others. Although both of the *"L"* models have very similar long-term gravity and SP trends, the short-term SP responses of the *"L-P"* and *"L-F"* models to shut-in are quite different. Since it is possible to measure long-term gravity changes with accuracy better than ~20 μGal using present-day repeat-survey technology (e.g. Sugihara, 2002) and to detect short-term SP changes within ~5 mV accuracy without sacrificing the low-cost advantages of SP techniques, a combination of long-term repeat gravity surveying and short-term continuous SP monitoring is believed to be a promising way to provide useful additional constraints in history-matching studies.

Outline of Field Experiments At the Okuaizu and Ogiri Areas

In 2002, GSJ started a collaborative research program called *"System Integration of Various Geophysical Measurements for Reservoir Monitoring"* to carry forward the NEDO/GSJ *"Development of Technology for Reservoir Mass and Heat Flow Characterization"* project. We are using multiple geophysical survey techniques to monitor field-wide shut-ins (usually associated with regularly-scheduled power station maintenance) in the operating Okuaizu and Ogiri geothermal fields in Japan.

In the Okuaizu field, we carried out continuous and/or repeat surveying of gravity and SP from March through November 2002 in cooperation with OAG (Okuaizu Geothermal) and Tohoku-EPCO (Tohoku Electric Power). During this time, a field wide shut-in took place (in March-April). We plan to do history-matching studies using these results, together with various reservoir engineering data (taken by OAG) and previous geophysical monitoring data (gravity by OAG/Tohoku-EPCO, 1994–1997; 1998–2002, gravity by NEDO and repeat SP by GSJ).

During the summer of 2002, various geophysical measurements (SP, gravity, GPS, tiltmeter and micro-earthquakes) were carried out in the Ogiri field. Simultaneously, short-term production tests involving new exploratory wells drilled in the adjacent Shiramizugoe area (just south of Ogiri) were in progress. In collaboration with NKG (Nittetsu-Kagoshima Geothermal), monitoring resumed in early March 2003 and is ongoing. In April 2003, the production rate was substantially reduced for Ogiri power station maintenance. We plan to carry out history-matching studies using these data, supported by various reservoir engineering data (provided by NKG) and earlier SP results (a 1987 SP survey by GSJ/NEDO and 1998–2002 continuous/repeat SP measurements by NEDO).

References

Horikoshi, T., Yamasawa, S., Ide, T. and Tosha, T. (2001), "NEDO's Project on Development of Technology for Reservoir Mass and Heat Flow Characterization. (1) Project Outline and Techniques to Improve the Reservoir Model", Geothermal Resources Council *Transactions*, v. 25, p. 641–644.

Ishido, T. and Pritchett, J.W. (1999), "Numerical Simulation of Electrokinetic Potentials Associated with Subsurface Fluid Flow," *J. Geophys. Res.*, v. 104, p. 15247–15259.

Ishido, T. and Pritchett, J.W. (2003), Characterization of Fractured Reservoirs Using Continuous Self-Potential Measurements , Proc. 28th Workshop Geothermal Reservoir Engineering, p. 158 165.

Ishido, T., Sugihara, M., Pritchett, J.W., and Ariki, K. (1995), "Feasibility Study of Reservoir Monitoring Using Repeat Precision Gravity Measurements at the Sumikawa Geothermal Field", *Proc. World Geothermal Congress 1995*, Florence, p. 853–859.

Pritchett, J.W. (1995), "STAR: A Geothermal Reservoir Simulation System," in *Proc. World Geothermal Congress 1995*, Florence, p. 2959–2963.

Sugihara, M. (2002), "Precise Gravity Monitoring with a FG5 Absolute Gravimeter, at the Yanaizu-Nishiyama Geothermal Field", Proc. 24th New Zealand geothermal workshop, p. 171 174.

Yamasawa, S., Tosha, T., Horikoshi, T. and Ide. T. (2001), "NEDO's Project on Development of Technology for Reservoir Mass and Heat Flow Characterization. (2) Geophysical Monitoring Techniques", Geothermal Resources Council *Transactions*, v. 25, p. 701–704.